Dynamical Processes of Orographic Cumuli II

1.   Summary of results of NSF-ATM-0444254 "Dynamical Processes of Orographic Cumuli", $460,473, 11/2005 – 10/2008. (http://www.atmos.uwyo.edu/~geerts/cupido/)

The present proposal builds on the CuPIDO field campaign, conducted during the summer of 2006 around the Santa Catalina Mountains in Arizona, and supported under NSF grant ATM-0444254. The CuPIDO (Cumulus Photogrammetric, In-situ and Doppler Observations) campaign was a remarkable success[1]. The University of Wyoming King Air (WKA) flew 16 missions, each targeting orographic cumuli and/or orographically controlled boundary-layer (BL) circulations. All in-situ probes and the airborne mm-wave Doppler radar, the Wyoming Cloud Radar (WCR)[2] performed well. We collected a total of 88 MGAUS soundings during the WKA flights. Ten ISFF stations operated continuously for 69 days, and two stereo-pairs of photogrammetric cameras collected digital images at 20 s intervals from sunrise to sunset (**Fig. 1**). CuPIDO was a joint effort between Joseph Zehnder's group and the University of Wyoming team. Dr. Zehnder is the PI for the stereo-photogrammetry, and he led the ISFF and MGAUS operations.

A survey of CuPIDO can be found in Damiani et al. (2008), which was featured on the cover of the January 2008 issue of the *Bull. Amer. Meteor. Soc.*. CuPIDO took place during a rather typical pre-monsoon dry period (22 June – 25 July) and an unusually wet monsoon period (26 July – 31 August) (**Fig. 2**b). Prevailing winds were generally weak (Fig. 2c) and the convective BL was deep, especially in the dry period (Fig. 2a). The WKA mainly sampled Cu congestus clouds, but the airborne sampling generally started at the Cu humilis stage. Thunderstorms were avoided by the aircraft. In terms of data wealth and quality, CuPIDO exceeded our expectations and is the P/I's most successful field campaign in his career to date.
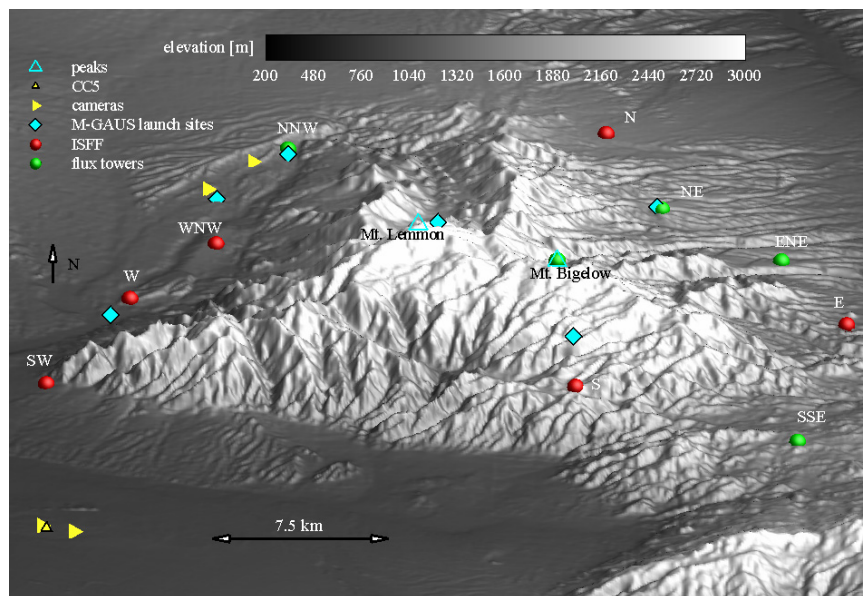

Fig. 1: CuPIDO layout around the Santa Catalina Mountains, about 25 km in diameter. The city of Tuscon stretches across the plains in the lower left of the image. Flux measurements (green circles) were made at four ISFF stations and at the Ameriflux tower on Mt. Bigelow (from Damiani et al. 2008).

ISFF: Integrated Surface Flux Facility (labelled according to their position to the mountain). **MGAUS**: Mobile GPS Advanced Upper-air Sounding system. **CC5**: 5th cloud camera, used for nowcasting.

Proposal ATM-0444254 listed two objectives:

Objective 1: "to examine spatial and temporal changes in the environment in which orographic

---

[1] All CuPIDO data, field catalog, and links are available at http://www.eol.ucar.edu/projects/cupido/.
[2] http://www.atmos.uwyo.edu/wcr/ - Section 4.1 provides more details about the WCR.

cumuli develop and decay, in order to gain insights into the synergy between towering cumulus convection and orographically-induced mesoscale circulations."

Objective 2: "to describe the WCR echo and kinematic structure of orographic cumuli at a scale of about 40 m, sufficient to resolve the primary entrainment processes; and to interpret this in light of microphysical and thermodynamic data, in order to gain new insights into the fundamental dynamical mechanisms controlling the evolution of cumuli."

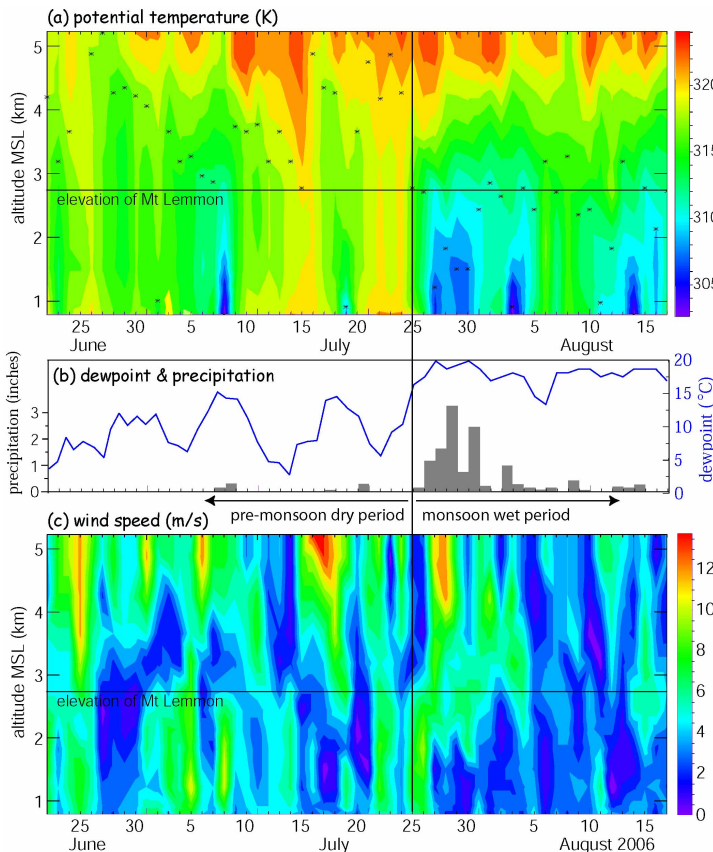## 1.1   BL circulations and orographic cumuli

Fig. 2: Time-height plots of (a) potential temperature and (c) wind speed for CuPIDO. The data are based on the 00 UTC TUS (Tucson, AZ) radiosondes. The stars in (a) indicate the depth of the well-mixed BL. The horizontal line shows the elevation of the top of the Santa Catalina Mountains. Also shown, in (b), are the 24-hr mean dewpoint and the average daily precipitation for the 10 ISFF stations.

Much progress has been made towards the 1st objective. Demko et al. (2008a) examine the evolution of mountain-scale mass, moisture and energy convergence, using both ISFF stations positioned around the mountain and 51 low-level flight loops around the mountain. They relate this to the evolution of BL depth (from soundings) and orographic cumulus depth (from photo-stereogrammetry). They find some evidence for a toroidal heat-island circulation, with divergence in the upper BL. Their three case studies suggest that growth spurts of orographic cumuli are not preceded by enhanced mountain-scale surface convergence, which suggests that these growth spurts are related more to BL heating over the mountain or to mid-tropospheric convective conditioning (e.g., Grabowski and Moncrieff 2004).

Geerts et al. (2008) use two months of ISFF, lightning and sounding data to study the diurnal variation of the mountain-scale surface convergence, its thermal forcing, and cumulus growth. The thermal forcing is examined in terms of a horizontal pressure gradient force, which is derived assuming hydrostatic balance. The daytime pressure deficit over the mountain, with a magnitude of 0.5-1.0 hPa, is hydrostatically consistent with the observed 1-2 K virtual potential temperature excess over the mountain. Geerts et al. (2008) also find that the consequence of deep convection (outflow spreading) is more apparent in the surface flow than its possible trigger (enhanced convergence). This study and Demko et al. (2008a) suggest that in mountains (unlike in plains) the BL convergence exerts little control over convective development. In fact the convergent flow advects cold air, and thus it is a negative feedback to surface heating over elevated terrain, and it reduces the moist static energy (MSE) of parcels over the mountain. At the same time the MSE convergence in the BL is essential for the maintenance of orographic convection. This interplay may explain the cyclic nature of orographic convection (e.g., Zehnder et

al. 2006; Demko et al. 2008a), with periods less than the duration of the daytime convective BL.

We are now proceeding with WRF (Weather Research and Forecasting) simulations of the interaction between BL processes and orographic cumulus development. Demko et al. (2008b) initiates WRF with composite soundings to examine the interaction between BL convergence and convective evolution, and the impact of CAPE, wind speed / wind shear, and soil moisture on orographic cumulus growth. The composites are subsets of CuPIDO's 69-day data period, based on some selection criteria. Four validation datasets are used, each in the form of a composite time series: orographic cumulus top height (from photo-stereogrammetry), mountain-scale surface convergence (from ISFF data), solenoidal forcing, and the horizontal pressure gradient force (the last two from ISFF plus Mt Bigelow data).

Demko et al. (2008c) compares WRF simulations with observations for the three case studies in Demko et al. (2008a) (**Fig. 3**), and discusses the impact of select BL schemes and cloud microphysical parameterizations on orographic circulations cumulus development. Cory Demko's PhD dissertation, to be defended in Fall 2009, will focus on the 1st objective of ATM-0444254.
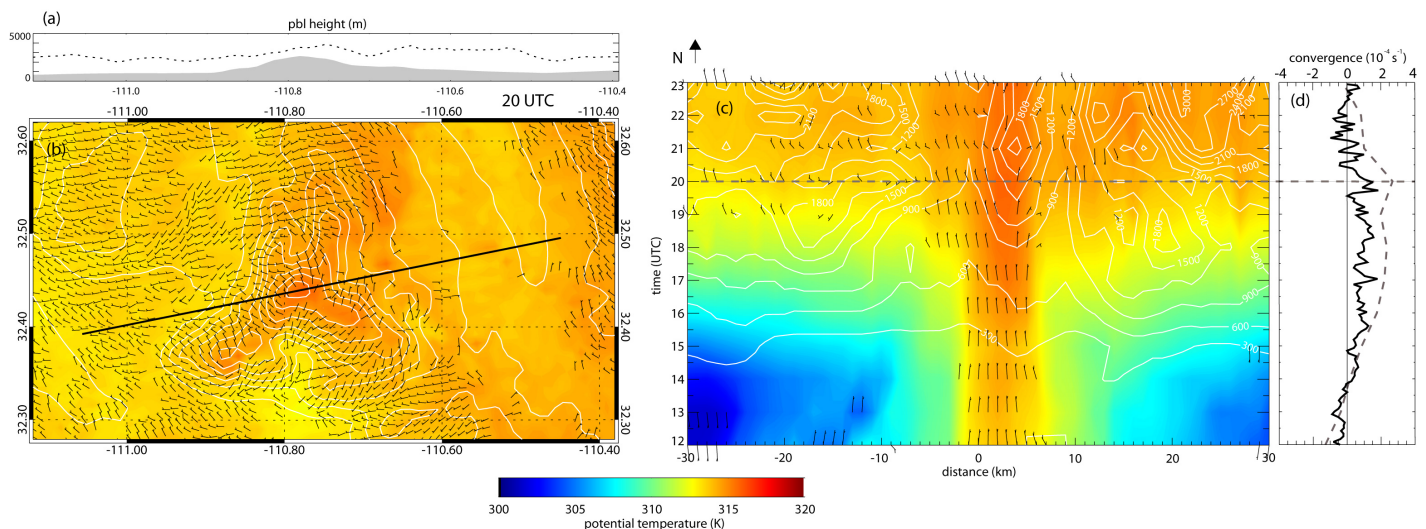

Fig. 3: WRF model (Δx = 1 km) output on 8/6/06: (b) surface winds (barbs – full barb is 10 kts; winds weaker than 2.5 kts are not plotted) and surface potential temperature θ (color) at 20 UTC. The topography is shown with white contours; the highest terrain is the warmest. (a) A cross-section of topography and BL depth above the terrain along the black line in (b), at 20 UTC. (c) A time-distance section of θ (color fill), BL depth (contours), and surface winds along the same section. (d) Time series of mountain-scale convergence of surface winds from the WRF simulation (dashed) and the ISFF stations (solid), for the same period as (c). The dashed line in (c) and (d) shows the time of map (a). Near dawn (12:30 UTC) a stable layer is present over the plains surrounding the Santa Catalina Mountains. At 20 UTC (0.5 hours after local solar noon) the surface flow clearly is convergent (d), and the warm pool within the convective BL over the mountain is dynamically consistent with this, i.e. the convergence is baroclinically forced. The BL domes over or just downstream of the mountain top (see (b)), thus BL thermals are most likely to reach the level of free convection there. By 20 UTC clouds have formed in the area where the BL is deepest, consistent with observations (from Demko et al. 2008c).

1.2   Fundamental cumulus dynamics

We have made progress with the 2nd objective as well, but we are learning that an in-depth analysis will require more effort than originally planned. Work to date has dealt with the basics. Progress in cumulus dynamics research has been hindered by inadequate measurements of <u>buoyancy</u>, <u>pressure perturbations</u>, and <u>entrainment</u>. Damiani et al. (2006) and Damiani and Vali (2007) use WCR data

collected in Cu congestus to shed new light on <u>entrainment</u>. They document upright and tilted toroidal (vortex ring) circulations around rising, buoyant cores and show that these circulations ingest much ambient air. An attempt to interpret Cu evolution in terms of the vertical profile of buoyancy was hampered by a lack of knowledge of the environment and macroscale structure of the sampled cumuli. This shortcoming was a key motivation for the CuPIDO campaign.

Wang and Geerts (2008) laid the foundation for improved <u>buoyancy</u> and entrainment estimates by questioning the accuracy of in-cloud temperature measurements. Both immersion and radiometric thermometers are challenged in cloud, for different reasons. A composite of the temperature variation near cumuli (**Fig. 4a**) highlights how uncertain buoyancy measurements are. Note that humidity measurements in-cloud are unreliable, thus it is generally assumed that cloudy air is saturated (i.e., a function of T only), so the uncertainty in cumulus buoyancy is largely driven by the uncertainty in temperature. Wang and Geerts (2008) used a physically-based empirical method to estimate the cold bias of reverse flow thermometers (RFT) in cloud. This bias, estimated at ~0.5 K on average, is due to evaporative cooling on a wetted sensor[3]. Wang and Geerts (2008) propose a correction inferred from the much stronger cold bias in the cloud exit region, using all good-quality Cu penetrations in three recent field campaigns, including CuPIDO. This correction makes the composite Cu buoyancy positive in RICO (as well as in CuPIDO), whereas the original RFT and the Ophir radiometric thermometer yield negative Cu buoyancy on average (Fig. 4a). The correction also reduces the entrainment rate: in **Fig. 4b**, for instance, the corrected w_{TOT} and θ_q are closer to ambient cloud-base values than the uncorrected ones.
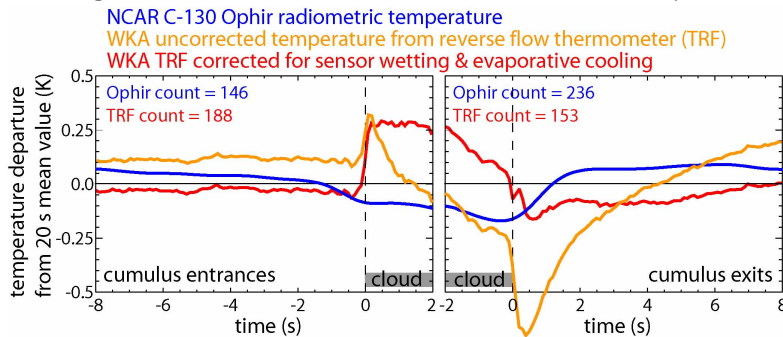
Fig. 4a: Composite temperature trace near all "clean" cumulus edges encountered by the NCAR C-130 and the WKA in RICO. Isolation and size criteria are used to define "clean" clouds (Wang and Geerts 2008), and each time series includes 8 s out of cloud and 2 s in cloud (grey belt). The temperature shown is a departure from the 20 sec mean value. Count = # of Cu in the composite.
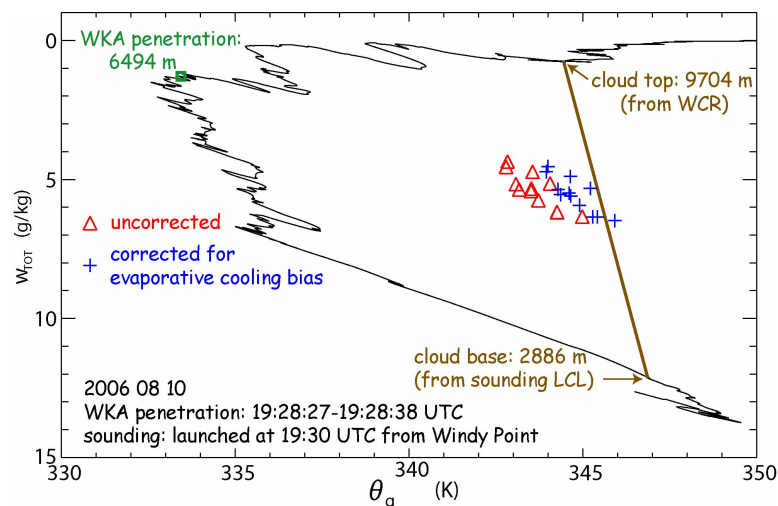
Fig. 4b: Impact of the Wang and Geerts (2008) temperature correction on entrainment. Plotted are θ_q, the wet equivalent potential temperature [defined in Paluch (1979)], and w_{TOT}, the total water mixing ratio, both conserved for pseudo-adiabatic moist processes. The correction affects both variables. The corrected in-cloud properties are closer to those at cloud base than the original ones, i.e. entrainment was overestimated.

Finally, Miao et al. (2008, in preparation) uses a novel technique to estimate <u>pressure perturbations</u> around Cu. Traditionally the accuracy of pressure perturbations measurements near convection has been limited by the uncertainty in the altitude of the aircraft (LeMone and Tartleton 1986; LeMone

---

[3] The reverse flow housing was designed to prevent wetting, but either some small droplets follow the reverse flow, and/or some water sheds from the rear of the housing in the turbulent flow and collects on the sensor. Because the air is dynamically compressed in the housing, it is sub-saturated even in cloud.

et al. 1988). Through differential GPS this uncertainty can now be reduced to O(0.1 m). Miao et al. (2008) compute the height of a constant-pressure surface near a level flight leg by vertically integrating the hydrostatic balance, following Rahn and Parish (2007) (Section 4.2). Perturbation pressure patterns around Cu congesti have been inferred from non-hydrostatic numerical simulations, and they can be interpreted in terms of dynamic and buoyancy forcings, but prior to CuPIDO they had not been measured in the field. Miao et al. (2008) document some patterns consistent with model output, but the main uncertainty has become the static pressure measurement aboard the aircraft. In collaboration with Thomas Parish and Alfred Rodi at the University of Wyoming, work is in progress to reduce this uncertainty, by applying corrections related to the airflow relative to the airframe. Thomas Parish is the PI on a separate NSF-funded campaign, Cloud-GPS, which involves more WKA penetrations in Cu. Both CuPIDO and Cloud-GPS data will be used to build and evaluate static pressure corrections.

Personnel for ATM-0444254:

When the grant commenced in Nov 2005, we started with Dr. Rick Damiani (Post-doc, 9 months) and Cory Demko (PhD student), as had been proposed. Following Damiani's unexpected departure in Jan 2007, we decided to split the post-doc support in a 50% post-doc (Dr. Qun Miao, 6 months) and a PhD graduate assistantship (Yonggang Wang). Both started in June 2007. Drs. Larry Oolman and Sam Haimov assisted us with the analysis of WKA and WCR data, respectively.

Completed papers under ATM-0444254:[4]

Damiani, R., J. Zehnder, B. Geerts, J. Demko, S. Haimov, J. Petti, G.S. Poulos, A. Razdan, J. Hu, M. Leuthold, and J. French, 2008: Cumulus Photogrammetric, In-situ and Doppler Observations: the CuPIDO 2006 Experiment. *Bull. Amer. Meteor. Soc.,* **89**, 57–73.

Demko, J. C., B. Geerts, J. Zehnder, and Q. Miao, 2008a: Boundary-layer energy transport and cumulus development over a heated mountain: an observational study. *Mon. Wea. Rev.,* accepted.

Geerts, B., Q. Miao, and J.C. Demko, 2008: Pressure perturbations and upslope flow over a heated, isolated mountain. *Mon. Wea. Rev.,* accepted.

Wang, Y., and B. Geerts, 2008: Estimating the evaporative cooling bias of an airborne reverse flow thermometer. *J. Atmos. Ocean. Tech.*, accepted.

Papers in preparation under ATM-0444254:

Miao, Q., et al., 2008: Airborne measurements of pressure perturbations in orographic cumulus. *Mon. Wea. Rev.*

Demko, J. C. et al., 2008b: Observations and simulations of the interaction between mountain-scale convergence and orographic convection. *Mon. Wea. Rev.*

Demko, J. C. et al., 2008c: Numerical simulations of boundary-layer solenoidal flow and cumulus convection over an isolated, heated mountain. *Mon. Wea. Rev.* [an early version of this paper appears as an Extended Abstract, presented at the AMS 13th Conference on Mountain Meteorology, 11-15 August 2008, Whistler, Canada, http://www.ametsoc.org/MEET/fainst/200813montmet17AP.html]

2.   Objectives and hypotheses

The key objectives of the present proposal mainly relate to 2nd objective of ATM-0444254:

1. to describe the observed fine-scale vertical and horizontal structure of the airflow and reflectivity fields within orographic Cu, inferred from the WCR, and to use this in combination with flight-level measurements and other CuPIDO data to learn about

---

[4] Unpublished papers can be accessed at http://www.atmos.uwyo.edu/~geerts/cupido/ .

a) fundamental Cu dynamics and microphysics, including updraft structure, toroidal circulation, the patterns and scales of entrainment, hydrometeor recycling, the process and effects of glaciation, Cu-scale buoyancy and perturbation pressure patterns, and their relation to ambient stability and wind shear;

b) the interaction of Cu with its immediate environment, in particular Cu detrainment and its impact on successive Cu development;

2. to use a high-resolution [$O(10^2)$ m], non-hydrostatic, cloud-resolving <u>model</u> with an adaptive horizontal grid (Grabowski and Smolarkiewicz 2002)

a) to statistically compare Cu properties (cloud water content, buoyancy, up- and downdrafts, pressure perturbations …), Cu entrainment patterns, and Cu detrainment patterns;

b) to use the spatially & temporally continuous and dynamically consistent model output to assist in the interpretation of the observations, in particular regarding Cu – environment interactions;

c) to examine, in a more idealized context, the vertical growth of orographic convection and its tendency to pulsate, under a range of observed ambient conditions, mainly wind speed, wind shear, & mid-level moisture.

Specific testable <u>hypotheses</u> associated with these objectives are as follows, respectively:

1. (based on measurements)

a) (fundamental Cu dynamics & microphysics)

i. (main hypothesis) Toroidal circulations surround the buoyant cores of growing Cu clouds. These circulations are essential to entrainment: significant entrainment occurs due to fine-scale instabilities at the updraft interface, and the mixed air is efficiently transferred to the Cu core by the toroidal circulation. Thus this circulation affects the drop size distribution and ice nucleation.

ii. The perturbation pressure field associated with relatively large, intense buoyant cores is measurable and its pattern is consistent with theory.

iii. Glaciation is sometimes rapid, and its effect on Cu dynamics, through added buoyancy, is measurable.

iv. Shear tends to tilt the vortex ring, and tends to concentrate compensating subsidence and detrainment in the downshear region. As Cu buoyancy vanishes upon reaching a stable layer, the vortex ring spreads out and weakens.

b) In places where a new Cu grows in the detritus of older Cu, Cu growth is enhanced, in particular in dry layers. This is a validation of the *moisture-convection feedback hypothesis* (Grabowski and Moncrieff 2004) at the scale of individual Cu towers.

2. (combining measurements with model output)

a) Observed PDFs of orographic Cu properties can be documented in unprecedented detail, and they compare well to modeled PDFs.

b) Model output can be used to refine conceptual understanding of Cu dynamics and Cu-environment interaction.

c) Model output can be used to understand the growth rate and pulsation of orographic Cu and to quantify the impacts of wind speed, wind shear, and mid-level moisture.

3. Significance

Shallow to deep convection is well-known to develop over mountains during the warm season where

the air is not too dry. The Santa Catalina Mountains serve as a natural laboratory for cumulus studies, given the spatially and temporally regular development of cumuli. Cumulus convection is of fundamental importance to the atmospheric circulation. It transfers moisture and momentum across isentropic surfaces in the troposphere and profoundly impacts the vertical profiles of humidity, stability, momentum, and radiative flux divergence. Also, it may yield most of the warm-season precipitation.

The growth of individual Cu towers and the interaction between adjacent or successive towers is poorly understood, and a number of conceptual theories exist[5]. Detailed observational evidence remains rather sparse. The combination of airborne in situ data with cloud radar measurements and photogrammetric data adds a new dimension to the study of cumulus dynamics.

Cumulus convection operates on a range of horizontal and vertical scales, and its finer scales cannot be resolved by operational numerical weather prediction (NWP) models. The ability of sufficiently resolved models to accurately predict the timing and intensity of daytime orographic convection primarily depends on the parameterization of two processes, i.e. turbulent exchange in the BL and cloud-microphysical processes. Single-column models are known to develop deep convection prematurely. 3-D cloud resolving models tend to capture the timing of convection better, although there is much disagreement amongst models (Grabowski et al. 2006). Orographic convection poses a special challenge, because of its coupling with the BL. If a model can accurately simulate the evolution of orographic convection under a variety of conditions, it can be expected to do well predicting cumulus evolution elsewhere.

4.   Novel observations of cumulus dynamics

4.1   Wyoming Cloud Radar

The WCR is a 95 GHz, multiple-beam Doppler radar. There are four fixed WCR antennas on the WKA, one oriented towards nadir, one looking ~30° forward of nadir in the vertical plane, one looking sideways <u>or</u> upward [depending on the position of a mirror in a faring on the aircraft frame], and one looking ~35° forward from the lateral beam in the horizontal plane (Damiani et al. 2006) (**Fig. 5**). The first two antennas allow dual-Doppler synthesis of the air motion in the vertical plane, a configuration referred to as vertical plane dual-Doppler (VPDD), illustrated in **Fig. 6**: along straight & level flight tracks, two beams view approximately the same sample volume from different directions, with time differences of the order of seconds, allowing dual-Doppler synthesis of the radial velocities in a plane below the aircraft (Damiani and Haimov 2006). The two antennas that point sideways, to the right of the aircraft, can be used for dual-Doppler synthesis in the horizontal plane (HPDD) (**Fig. 7**). While there are antennas looking in both vertical directions, allowing for a full profile of reflectivity and vertical velocity in a section centered at flight level (Fig. 5b), the WCR can look in one horizontal direction only, to the right of the flight track.

In CuPIDO a WCR range resolution of 37 m was generally used. The minimum detectible signal was about -25 dBZ at a range of 1 km and about -16 dBZ at 3 km. For strong echoes we used all four WCR antennas simultaneously, but for weak echoes we only used the most relevant antenna(s), to gain some sensitivity. The echo from shallow warm Cu tended to be at the margin of WCR detectability at close range. Cloud droplets are much smaller than ice particles, so WCR reflectivity

---

[5] These conceptual theories are reviewed in Section 3.1 of the ATM-0444254 proposal, available at http://www.atmos.uwyo.edu/~geerts/cupido/

increases dramatically upon glaciation. WCR reflectivity profiles from successive penetrations, only a few minutes apart, indicate that rapid glaciation was common in CuPIDO.
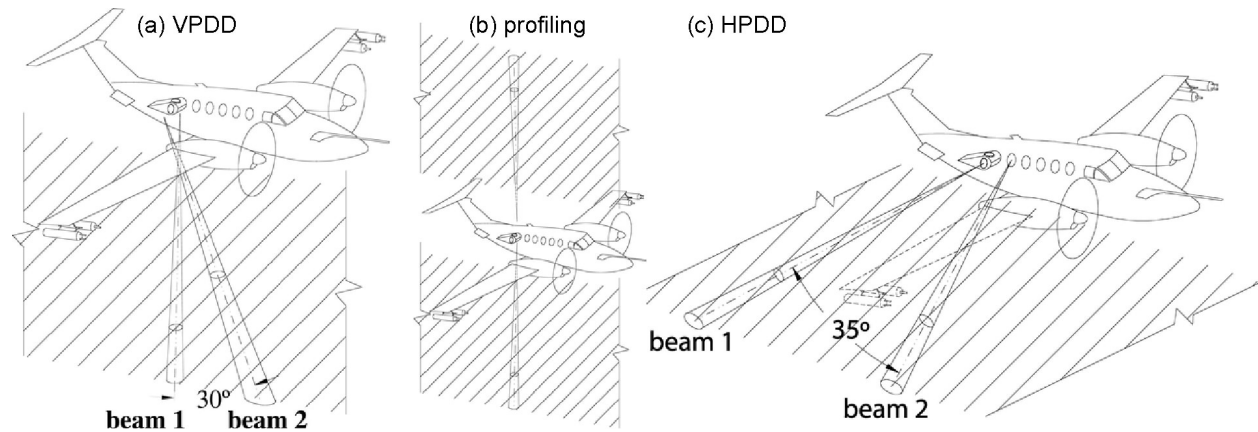

Fig. 5: WCR antenna options aboard the WKA (from Damiani et al. 2006; Damiani and Vali 2007).
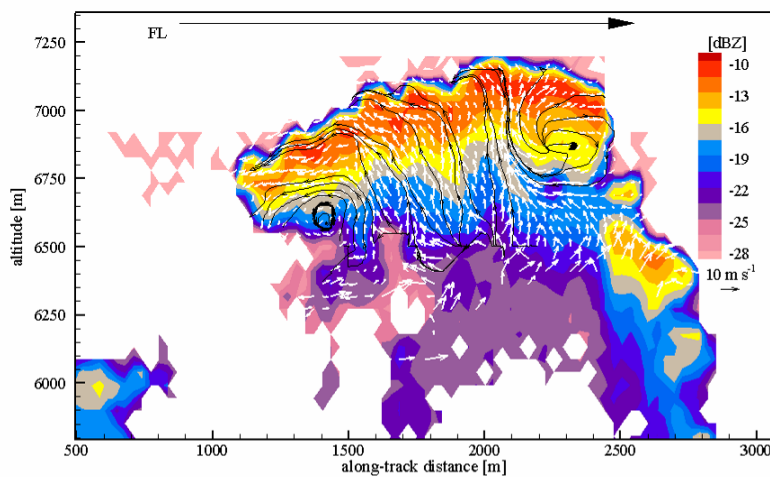

Fig. 6a: VPDD analyses of a Cu tower sampled on 10 August 2006 at 1751 UTC. Note the mushroom appearance and the intense toroidal circulation with intrusions of presumably dry air (reduced reflectivity) at the base of the tilted vortex ring. (FL=flight level)

Fig. 6b: Photo of the Cu tower, taken from the downshear side about 1 min before the WCR transect in Fig. 6a. The flight track remains just to the right of the highest top in the photo.
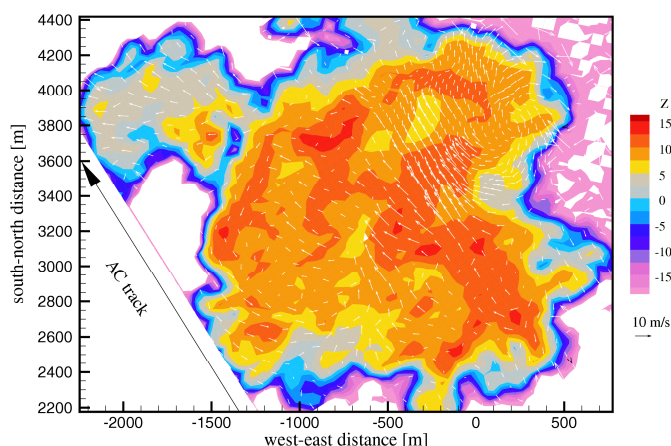

Fig. 7: Example of a horizontal-plane dual-Doppler (HPDD) analysis of a Cu congestus containing ice (31 July 2006).

Previous observational studies of cumulus dynamics were hampered by the complex 3-D structure and rapid evolution of Cu. Until recently airborne analyses have entirely relied on 1-D (flight-level) data (e.g., Blyth and Latham 1993). Cumulus research using ground-based X- to S-band Doppler radars (e.g., Knight et al. 2002) can describe the echo volume at high temporal resolution, but these radars may be affected by Bragg scattering and mainly see the outcome of convection (i.e. the precipitation), not the

cumuli themselves. Damiani et al. (2006) demonstrate the capabilities of the WCR airborne configuration in providing a more complete spatial view of cumuli, in terms of both small-scale and cloud-scale dynamical features.

Given the rapid evolution of cumuli, it is difficult to relate a sequence of aircraft penetrations to cumulus evolution. In CuPIDO the winds were generally light (Fig. 2) and we often aligned the flight track with the mean wind and repeated the ~20 km long tracks in opposite directions. Consecutive WCR transects were used to identify two, sometimes three snapshots of a single, evolving Cu tower. This enables us to interpret in-situ data in the context of the Cu lifecycle (**Fig. 8**). Temporal evolution is particularly important in testing the moisture-convection feedback hypothesis (1.b).
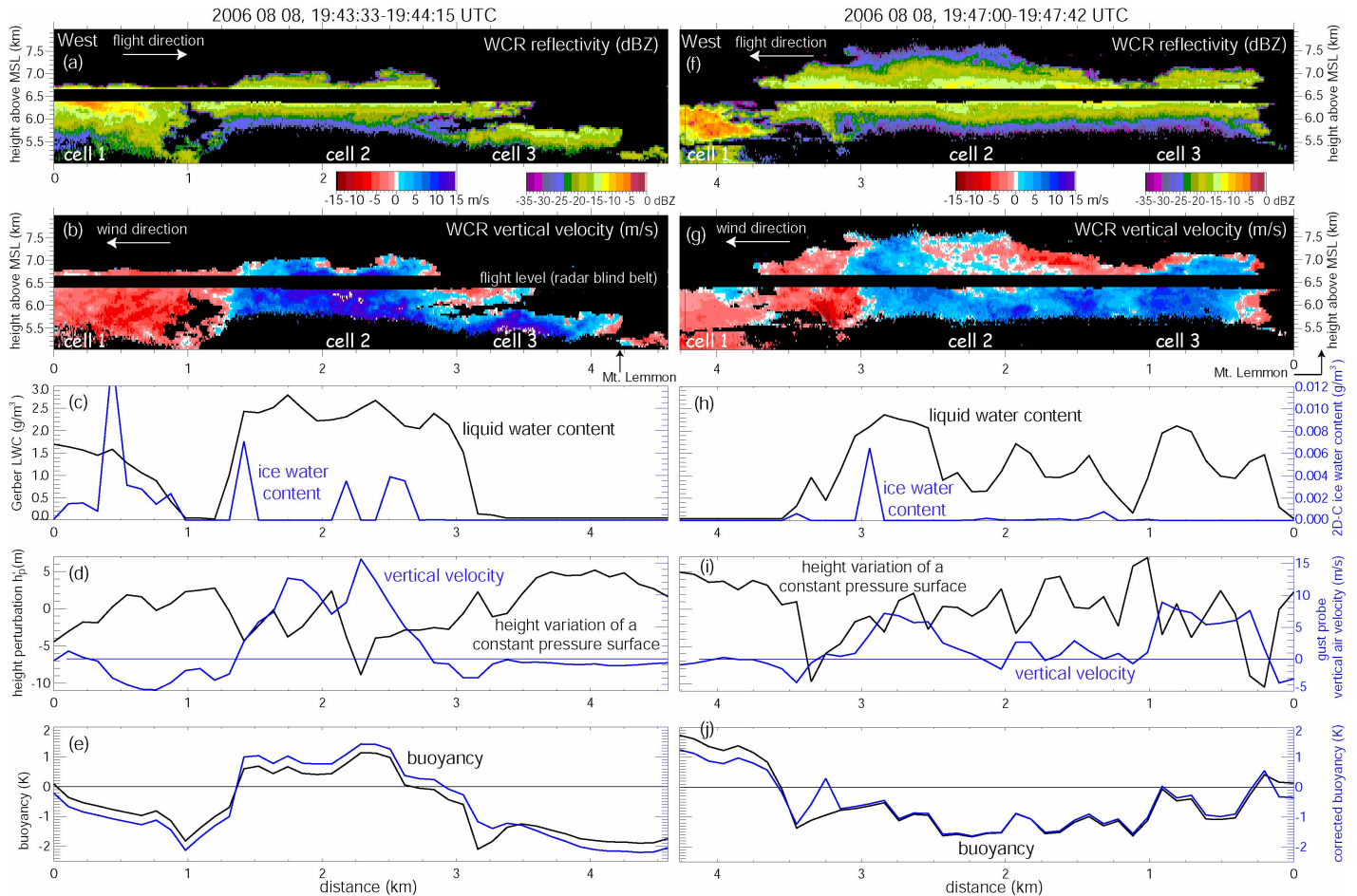

Fig. 8: An illustration of combined WCR-WKA data display for three adjacent Cu cells in CuPIDO on 08/08/2006. The left panels depict a transect collected about 3 min before that on the right. The upper panels (a,f and b,g) are WCR profiles centered at flight level. The horizontal axis is stretched by a factor of 3 relative to the vertical axis. The lower panels (c-e and h-j) depict flight-level data. The "corrected buoyancy" (blue line) is based on the reverse flow temperature correction proposed by Wang and Geerts (2008). This correction tends to increase the buoyancy in young cells. Cell 1 is the oldest, cell 3 the youngest. All cells formed over Mt Lemmon, located on the upwind side near the right edge of the transects, as indicated. Cell 1 is glaciating and collapsing. Cell 2 is buoyant and rapidly ascending in the 1st transect, but negatively buoyant and starting to collapse 3 min later. At both times cell 2 is mostly liquid, with very high supercooled water concentrations. Cell 3 is below flight level in the 1st transect; the strong updraft and the high at flight level suggest that it is buoyant at this time. Three min later it has penetrated through flight level (-15°C), but it shows no sign of glaciation yet. In the next three transects (4-11 min later, not shown) cells 2 and 3 merge further and glaciate.

WCR data will be used mainly to examine the presence and diversity of vortex-ring type structures in the ascending cloud-caps. The toroidal circulation is important because it appears to be the key player in Cu entrainment (Blyth et al. 1988; Damiani et al. 2006; Section 6.1). It may directly affect drop size distribution and precipitation development. It displaces hydrometeors towards the sides of the updraft, initiating a spatially preferential arrangement of particles, and it may recycle hydrometeors back into the thermal core (Fig. 6a). Also, ice crystals may grow rapidly through the Bergeron process or by riming if the vortical dynamics drive ice crystals back into a saturated updraft region. We can examine this since along select WKA flight tracks, i.e. where the track intersects a WCR particle re-ingestion signature.

4.2   Combining flight-level with remotely-sensed observations

The combination of flight-level data with vertical profile WCR data (e.g., Fig. 8) is far more powerful for Cu dynamics research than in situ flight-level data alone. The perturbation pressure field shown in Fig. 8 is derived as follows: the geopotential height (h_p) of a reference pressure level (p_{ref}) in the vicinity of a flight level is computed as
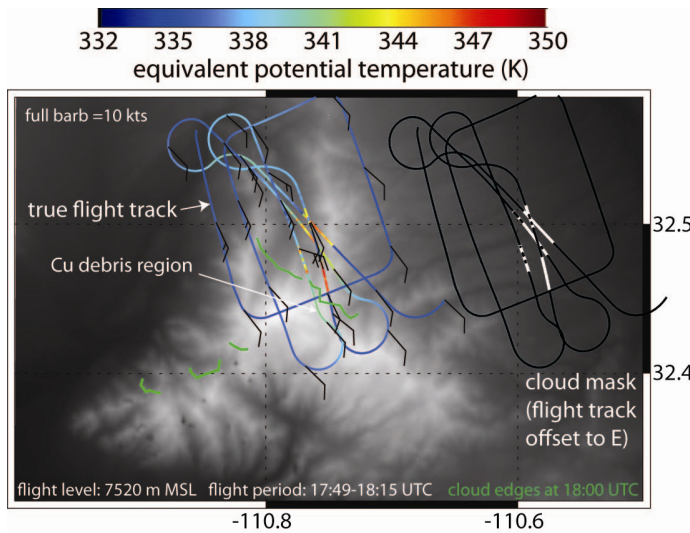

Fig. 9: WKA flight track colored by in situ θ_e, in situ winds (barbs), and flight-level cloud edges (green lines) as determined by the camera stereo-pair to the southwest of the mountain (Fig. 1). The background map shows topography. The in situ cloud mask (white sections along the black offset track) is based on a FSSP cloud droplet concentration threshold of 25 cm^{-3}.

$$h_p = z_{ac} + \frac{R_d}{g} \int_{p_{ref}}^{p_{ac}} T_v\, d\ln p$$

where R_d is the ideal gas constant for dry air, g is gravity, and T_v is the virtual temperature. Pressure perturbations (p) can then simply be inferred from the variations in h_p:

$$p' = \rho g\left(h_p - \overline{h}_p\right)$$

where $\overline{h}_p$ is the average geopotential height over some domain, and ρ air density. Since the flight track is relatively level, the range of the integral bounds is small, and flight-level measurements of T_v can be used. The height of the aircraft z_{ac} is computed very precisely using differential GPS. The largest uncertainty turns out to be in the static pressure (p_{ac}) measurement. The perturbation height h'$_p$ varies by ~10 m (equivalent to ~1.0 hPa) in a complex way in Fig. 8; e.g., two lows appear to surround the merging cells 2 and 3 (Fig. 8i, at x=3.3 and x=0.3 km). They may mark the centers of a broad vortex ring. The buoyancy field in Fig. 8e,j includes all terms, i.e. water vapor, water loading and pressure perturbation terms (e.g., eqn 2.50 in Houze 1993); for convenience, it is expressed in units of temperature (K).

An example of combined flight-level and photogrammetric cloud edges is shown in **Fig. 9**. The Cu patches contain high θ_e (equivalent potential temperature) values; higher θ_e values occur downstream of the Cu (to the NW) compared to upstream, indicating that the sampled Cu (or, more likely, its predecessors) detrain air rich in moist static energy into the environment at this level.
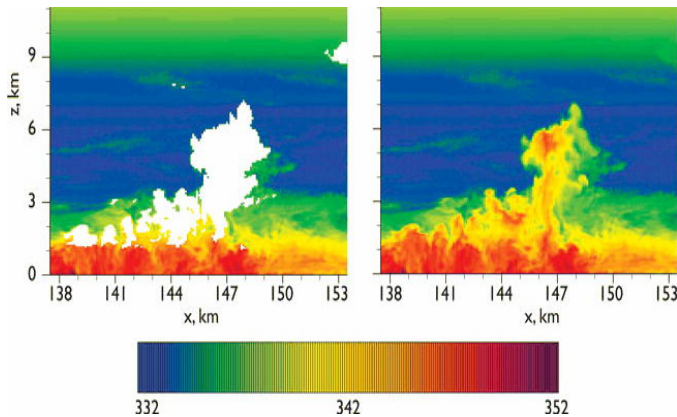
10

Fig. 10: *Cross section of θ_e for a mature Cu congestus (from Khairoutdinov and Randall 2006). The white region in the left panel is a cloud mask. The cloud appears to be detraining to the right at mid-levels.*

There is also a patch of θ_e-rich, clear air just west of the cloud edge close to the mountain peak, marked as "Cu debris region" in Fig. 9, as a Cu had recently collapsed there. The data in Fig. 9 can be compared with the θ_e distribution around a simulated Cu congestus (**Fig. 10**). We plan to compare the evolution of Cu growing in θ_e enriched air to that in unmodified ambient air, through observations and modeling. It can be argued that, for orographic convection emerging from a geographically-fixed point, the wind has to be very weak, such that the advective timescale is longer than the Cu lifespan, but in the case of the Santa Catalina Mountains the flow was southeasterly on several flight days, roughly along the 12 km long ridge between Mt Bigelow and Mt Lemmon (Fig. 1). Convection regularly developed along that ridge, and decayed downstream of Mt Lemmon (Fig. 8).

5. EULAG model

The model to be used in this study is the massively-parallel all-scale anelastic non-hydrostatic semi-Lagrangian/Eulerian model EULAG. The model applies terrain-following coordinates and the non-oscillatory forward-in-time (NFT) integration scheme (Smolarkiewicz and Margolin 1997). EULAG has been applied over the last decade or so to a diverse range of geophysical fluid dynamics problems, from microscale processes (direct numerical simulations; Andrejczuk et al. 2004; 2006), through small-scale atmospheric dynamics (large-eddy simulations; e.g., Margolin et al. 1999; Slawinska et al. 2008), deep convection and its coupling with the large-scale dynamics (e.g., Grabowski et al. 2000; Grabowski and Moncrieff 2001, 2003), up to atmospheric general circulation simulations (Smolarkiewicz et al. 2001; Grabowski and Smolarkiewicz 2002; Prusa and Smolarkiewicz 2003). The model has a wide suite of microphysical parameterizations, from simple single-moment bulk microphysics (for warm-rain and ice processes; Grabowski 1998), through a more sophisticated double moment ice scheme (Grabowski 1999) and recently-developed double-moment warm-rain and ice schemes (Morrison and Grabowski 2008a, b). EULAG can also run with a bin microphysics scheme developed by Grabowski and applied in Morrison and Grabowski (2007) and Grabowski and Wang (2008). The model also features a sophisticated representation of turbulent mixing (Grabowski 2007); its coupling to the double-moment microphysics scheme presently is under development.

A unique feature of EULAG is its highly sophisticated grid adaptivity in the horizontal (Prusa and Smolarkiewicz 2003; Prusa and Gutowski 2007). This will allow applying a very high resolution over the highest terrain, where vertical transport is concentrated, an elevated convective BL forms, and clouds develop. Here we can apply a horizontal gridlength of 50m or less. Away from the mountain a gradually coarsening resolution is employed, with a horizontal gridlength of ~500m near the domain edge. A high vertical resolution (say, gridlength of 50m) will be used over the entire computational domain to best represent the BL evolution over the mountain. The simulations will be initialized using a pre-convective MGAUS sounding; later soundings (during convective activity over the

mountain) will be used to evaluate the model and to study the interaction between convection and its environment.

With this approach, a computational domain of 40km by 40km will cover the entire mountain range and allow relatively inexpensive simulations of multiscale processes associated with convection development and evolution over the mountain. In particular, such a setup will simulate the development of mesoscale circulations due to daytime surface heating that result in the eventual formation of convective clouds. At the same time, the vertical and horizontal resolutions in the center of the domain will be high enough to faithfully represent individual Cu turrets, the coarser-scale entrainment processes, interactions between clouds and temperature and/or moisture inversions as well as between Cu developing in succession. The WRF model (which we are using to describe the mountain-scale BL circulation and gross convective evolution, see Section 1.1) is not designed to resolve processes at the scale of individual Cu turrets.

6.   Research questions

6.1   Observations of Cu dynamics

Our first objective deals with the fine-scale kinematics and dynamics of Cu, and its effect on the environment. Convection is driven by buoyancy which depends on latent heating and ambient stability. Condensational heating is strongly controlled by vertical motion; freezing depends more subtly on cloud and aerosol microphysics. Cu clouds entrain ambient unsaturated air, which limits growth, esp. for narrow towers. Blyth (1993) and Zhao and Austin (2005) present a thorough review of cumulus entrainment studies. Other factors complicate the study of convection. Cu is believed to grow mainly on the upshear side and detrain on the downshear side (e.g., Perry and Hobbs 1995). Many Cu towers probably start as thermals in the convective BL. The details of the initial disturbance profoundly affect the convective evolution (e.g., Johari 1992). Atmospheric turbulence in the inertial subrange due to BL convection and the Cu updraft affects Cu evolution. The outcome is a series of possible behaviors that can hardly be classified as a 'bubble' [Scorer (1957), refined into a buoyant vortex ring (Turner 1957)] or a 'plume' (Stommel 1947; Squires 1958). Observations of pulsating Cu in CuPIDO and over plains (e.g., French et al. 1999) suggest a bubble character, not unlike thermals in the convective BL. The lifespan of a Cu tower, even an airmass thunderstorm, is comparable to the time required for a parcel to rise from its source to its buoyancy equilibrium level (Doswell 2001), although Cu towers often occur in longer-lived clusters.

Field observations have demonstrated that mixing is likely to occur near the cloud top (e.g., Paluch 1979, Betts 1982), but it cannot be confined to the cloud top. Blyth et al. (1988) and Blyth (1993) describe Cu as shedding thermals, with entrainment occurring near the ascending cloud-top and mixed parcels descending around the edges of the thermal updraft core. Damiani et al. (2006), using WCR/WKA data collected in Wyoming, generally confirmed this model, and emphasized the entrainment below the cloud top vortex ring. It appears that buoyancy reversal and penetrative downdrafts are more likely to be the effect and not the cause of entrainment. Cooper and Rodi (1982), examining the statistical properties of droplet spectra and air velocity data in summer cumuli, depict mixing as a highly inhomogeneous process occurring first at cloud top. The result is pockets of negatively buoyant fluid, some of which penetrate into the rising thermal. Some of these pockets are not ingested, but remain at the edge of the updraft, where they trigger downdrafts. Yet some descending parcels may still be recaptured in the wake of the buoyant core. Water tank experiments by Johari (1992) confirm the hypothesis of a toroidal circulation that causes ambient

fluid to be entrained from the bottom of the ascending parcel. This overturning process may aggregate negatively buoyant air at the bottom of the rising core, leading to deep downdrafts.

Klaassen and Clark (1985) and Grabowski and Clark (1993) use numerical simulations to conclude that buoyancy reversal following evaporative cooling only plays a minor role in the generation of downdrafts, compared to dynamical effects. Blyth et al. (1988) identify the thin mixing region immediately above the ascending cloud top as the main entrainment source region; in their model, the mixed parcels descend along the edges of the thermal core into the turbulent trailing wake. Jonas (1990) and Stith (1992) support the idea of lateral mixing following the transport of environmental air from the cloud top via thin subsiding layers.
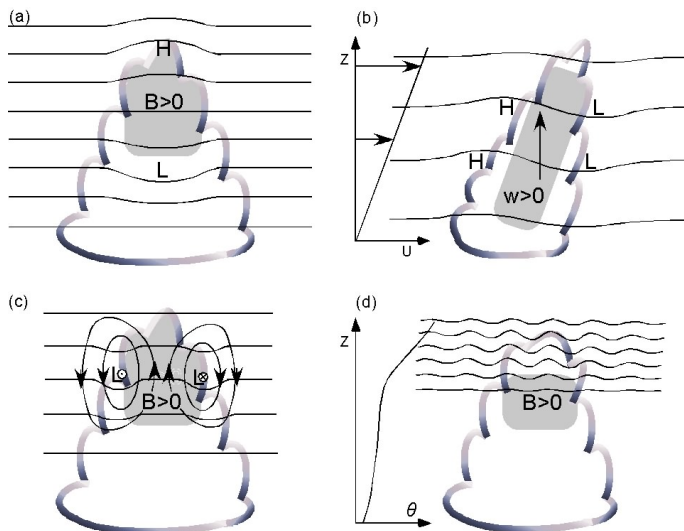

Fig. 11: Schematic perturbation pressure patterns associated with Cu convection, in vertical cross sections. The horizontal lines are isobars, B is buoyancy, u wind speed, w vertical velocity, and θ potential temperature.

Non-hydrostatic pressure perturbations, as shown in Fig. 8, occur in response to the buoyancy forcing and the resulting updraft. For instance, a high can be expected on the upshear size of an updraft, and a low on its downshear side (**Fig. 11**b) (e.g., Houze 1993, p. 290; Barnes 1995; Doswell and Markowski 2004). A vortex ring may correspond with a low-pressure ring (Fig. 11c) and gravity waves may propagate horizontally and vertically under suitable ambient stability (Fig. 11d) (e.g., Nicholls and Pielke 2000). The perturbation pressure field in turn largely controls the environment's flow response to convection (e.g., Zhang and Wu 2003), including vertical drafts and entrainment. We may be able to use p' as an independent measure of the intensity and size of a buoyant core or an updraft. For instance, a high can be seen above the emerging cell 3 at x=3.5 km (Fig. 8d). Since this tower is below flight level, we do not have in situ buoyancy data, but the strength of the high suggests that this updraft is quite buoyant (Fig. 11a) (e.g., Houze 1993, p. 223).

The following is a list of intertwined questions. Our CuPIDO analysis is expected to address them all. We cannot expect this analysis to yield definitive answers, but we hope to gain some insights. The questions are organized following the list of objectives in Section 2.

- The combination of WCR and flight-level data will be used to describe characteristic Cu growth patterns; this will allow us to address a number of linked questions related to **fundamental Cu dynamics and microphysics**:

  o What <u>conceptual model</u> best describes the growth stages of a convective cloud? Does the shedding thermal model (Blyth 1993) apply, and if so, does it need to be refined?

  o Is a growing Cu generally marked by an ascending, buoyant core surrounded by a horizontal or tilted <u>vortex ring</u>? A toroidal circulation implies that the core's updraft speed [from WCR] exceeds the cloud-top ascent rate [from photogrammetry]. The difference between the former and the latter velocities is a measure of the circulation rate, which is related to

the mass entrainment rate.

- How is the <u>recycling of hydrometeors</u> by a vortex ring (e.g., Fig. 6a) affected by the depth and strength of the buoyant core? How does this re-ingestion affect the particle size distribution, precipitation growth, and the onset of glaciation? The WCR reflectivity and flow fields may reveal clues about hydrometeor advection and growth/decay in specific sectors of the cloud.

- What processes lead to <u>glaciation</u>? Successive WCR reflectivity transects reveal rapid glaciation. In some CuPIDO cases high WCR reflectivity and flight-level ice were observed near the cloud edge. Dye et al. (1986a, b) and Hobbs and Rangno (1985) report that the largest concentrations of ice particles tend to occur at the edges of the updrafts and near the cumulus summits (as is the case for Fig. 6a). The intense small-scale turbulence along the cloud edge may enhance ice nucleation, due to lower temperatures and higher supersaturation within vortices. This ice may then be carried into the buoyant core by the toroidal circulation. A related question is whether the sudden latent heat release by freezing has a measurable dynamical impact.

- Where and at what scales does <u>entrainment</u> occur? How do WCR entrainment signatures and scales vary with buoyancy and updraft strength? Are small-scale vortices at the top and sides of the main updraft [due either to cloud-top instability (Grabowski and Clark 1993) or to the interfacial shear] resolvable by the WCR? Such vortices generate turbulent kinetic energy and may affect the cloud-scale entrainment rate. Are Cu congesti more inhomogeneous near their buoyant top (due to the toroidal circulation, leaving the least diluted air found within the vortex ring), and more homogenous in the lower cloud region marked by smaller buoyancy and weaker updrafts?

- The CuPIDO dataset uniquely enables <u>pressure perturbations</u> to be measured with an estimated accuracy of $O(0.1$ hPa$)$. Thus the basic question can be addressed, for the first time, whether the observed spatial patterns of p' are consistent with theory and numerical simulations (e.g., Nascimento and Droegemeier 2006).

- How does vertical <u>wind shear</u> affect fundamental Cu dynamics? Shear appears to tilt ring vortices in the upshear direction, because of an aerodynamic torque (Damiani and Vali 2007). How does shear, and associated cloud-scale pressure perturbations, affect the flow field and entrainment processes in Cu congestus? Cloud-level wind shear was generally weak in CuPIDO, but the WKA sampled two moderate-shear cases.

- The CuPIDO data will be further used to address questions related to **Cu-environment interaction**:

  - Is the combined WKA and stereo-photogrammetric dataset sufficient to describe patterns of <u>detrainment</u> of moisture, θ_e, and momentum?

  - Does the detrainment of cloudy air and/or the collapse of a Cu tower produce an environment in which successive Cu can grow deeper (<u>moisture-convection feedback</u>)? On several CuPIDO days (e.g. 8/17/06) orographic Cu grew stepwise, held back for some time below one or more stable layers (Damiani et al. 2008). Profiles of θ_e from successive MGAUS soundings and aircraft data will be used to determine whether the stable layer was eroded by convective debris, or whether the BL θ_e became large enough for later convection

to penetrate the stable layer.

- o Is the <u>pulsating</u> nature of orographic convection (e.g., Demko et al. 2008a) driven by the interaction between Cu evolution and BL circulations around the mountain?

- Many of these questions will be addressed further through **simulations of Cu dynamics**. Observations are very limited in time and space compared to model output. We will use the dynamically consistent model output to assist in the interpretation of the observations. The main model-related questions regard the vertical growth of orographic convection, the moisture-convection feedback, and the pulsating nature of convection:

  - o What controls growth through a stable layer? Is a stable layer eroded by compensating subsidence near the cloud top or by detrainment of θ_e-rich air? What is the effect of shear, which inhibits Cu growth through the remnants of previous Cu because the detrained material is advected downstream?

  - o What controls growth through a dry layer? How is buoyancy reverse in a model cloud that resolves entraining circulations? Is penetration through the dry layer only possible through debris of older Cu? Are the results sensitive to microphysics and representation of buoyancy reversal due to subgrid-scale mixing?

7.   Proposed research schedule

<u>Year 1</u>: Demko et al. (2008b), Demko et al. (2008c), and Miao et al. (2008) will be submitted and reviewed, and Cory Demko will prepare his PhD dissertation. All WCR data need to be reprocessed to reduce noise and remove close-range cross-antenna leakage. Objectives 1(a)-(b) will be pursued using WCR single- and dual-Doppler analyses, combined with in situ measurements, derived in situ variables (buoyancy, pressure perturbation), and other CuPIDO data. We will develop the Eulag model configuration (Objective 2) and examine how PBL schemes and cloud microphysics schemes affect the timing and growth rate of convection over the Santa Catalina Mountains.

<u>Year 2</u>: Both Objectives 1 (observations of Cu dynamics) and 2 (simulations of Cu dynamics) will be pursued, in parallel, with talks/posters to be presented at meetings such as AGU meetings, the ICCP (International Convention on Clouds and Precipitation), the AMS Conferences on Radar Meteorology and Mountain Meteorology, and AGU meetings, and papers to be submitted to *J. Atmos. Sci.*, *Mon. Wea. Rev.*, and *Quart. J. Roy. Meteorol. Soc.*.

<u>Year 3</u>: Continuation of Objectives 1 and 2 and completion of publications; preparation of the educational initiative (Section 8); preparation of a future proposal, building on our CuPIDO work. And Yonggang Wang hopes to defend his PhD dissertation in Year 3.

8.   Educational initiatives

This proposal will support doctoral work for two PhD candidates, Cory Demko and Yonggang Wang. Our CuPIDO research is providing excellent materials for an educational module on orographically-controlled, thermally-forced circulations and orographic convection. The PI is giving an overview of this topic at a workshop preceding the AMS 13th Conference on Mountain Meteorology in August 08. We plan to discuss the development of such module with the UCAR COMET group, possibly in collaboration with James Steenburgh and/or Dave Whiteman, both at the U. Utah.